JMATPRO	Journal of Advanced Materials and Processing 10 (2): 3-10, Spring 2022 http://jmatpro.iaun.ac.ir 20.1001.1.2322388.2022.10.2.1.6

Research Paper

Investigation of Microstructure and Mechanical Properties of Ni-Cu-P Coatings Deposited by the Electroless Method

Danial Davoodi[1], Amir Hossein Emami[1,*], Sayed Mahmoud Monir Vaghefi[2], Mahdi Omidi[1], Hamid Reza Bakhsheshi-Rad[1]

1. Advanced Materials Research Center, Department of Materials Engineering, Najafabad Branch, Islamic Azad University, Najafabad, Iran.
2. Department of Materials Engineering, Isfahan University of Technology, Isfahan 84156-83111, Iran.

ARTICLE INFO

Article history:

Received 21 February 2022
Accepted 30 March 2022
Available online 1 April 2022

Keywords:
Electroless Ni-Cu-P
Microhardness
L80 steel
TEM
Heat treatment

ABSTRACT

In the current study, the effect of colloidal copper nanoparticles on the deposition rate and hardness of Ni-Cu-P coating deposited by electroless method on L80 steel substrate was investigated. Copper particle size, microstructure, chemical composition, and hardness of the coating before and after heat treatment at different temperatures were examined by transmission electron microscopy (TEM), X-ray diffraction (XRD), scanning electron microscopy (SEM) equipped with energy dispersive X-ray (EDS) analysis, and microhardness. The microstructure study by XRD showed that the Ni-Cu-P coating has an amorphous structure. The heat treatment at 400 °C transformed the structure from amorphous to crystalline and formed Ni_{α}, Ni_3P, and $Ni_{3.8}Cu$ phases. The amount of copper nanoparticles in the coating 4.58 wt% was measured. The deposition rate of the Ni-Cu-P coating was 11 µm/h. Furthermore, the hardness of the coating increased from 738HV to 1300HV by performing heat treatment.

Citation: Davoodi, D.; Emami, A.H.; Monir Vaghefi, S.M.; Omidi, M.; Bakhsheshi-Rad, H.R. (2022). Investigation of Microstructure and Mechanical Properties of Ni-Cu-P Coatings Deposited by the Electroless Method, Journal of Advanced Materials and Processing, 10 (2), 3-10. Dor: 20.1001.1.2322388.2022.10.2.1.6

* **Corresponding Author**
E-mail Address: Dr.s.a.h.emami@gmail.com

1. Introduction

L80 steels, due to the desired mechanical properties and low price, are widely used as casing and tubing of pipes in gas and oil wells according to API5CT standards. However, these steels do not have good corrosion resistance [1–3].

Today electroless Ni-P coatings are widely used to increase the corrosion resistance of ferrous and non-ferrous metals. Excellent corrosion resistance, good wear behavior, and high hardness have led to the increasing use of electroless Ni-P coatings, especially in the oil and gas industry [4–6]. Over the years, researchers have been trying to optimize the properties of coatings parameters such as temperature, pH, concentration, and chemical composition of electroless baths and the rate of deposition. Furthermore, compositing these coatings with metal and ceramic particles upgrades the mechanical and chemical properties of the coatings [7–9].

Recently, studies have been performed on electroless Ni-P coatings composite reinforced with MoS_2, ZrO_2, SiC, Al_2O_3, PTFE, Ti, and Mo [10–15]. Unlike electrical coating methods, electroless coating methods have a lower deposition rate, increasing coating time and costs [2,16]. In electroless baths, different crystallographic structures from amorphous to crystalline states can be obtained by changing the two parameters of temperature and pH. Also, in electroless baths with acidic pH, the deposition rate can be increased to some extent by increasing pH and temperature simultaneously. On the other hand, failure to control these two parameters can lead to the decomposition of the electroless bath. Therefore, by changing the chemical composition and using other chemical factors such as deposition rate accelerators, in addition to increasing the deposition rate, other parameters such as hardness and corrosion resistance are also increased [17].

Tabatabai et al. [18] investigated the effect of different amounts of sodium sulfate (Na_2SO_4) in an electroless acid-coated bath on the deposition rate and corrosion behavior. The results showed that the deposition rate in the bath without Na_2SO_4 was 10 µm/h, while at an optimal concentration of 1 g/LNa_2SO_4, the deposition rate reached 14 µm/h. On the other hand, the corrosion current density decreases from 3.3 µA/m^2 in the bath without Na_2SO_4 to 1.3 µA/m^2 in the bath with 1 g Na_2SO_4, due to the reduction of cavities and defects in the coating and surface passivation. Kundu et al. [19] reported that the addition of tungsten sulfate in Ni-P electrolysis solution significantly increased the hardness due to the formation of a solid solution between W and Ni elements in the electroless Ni-P-W coating before heat treatment and also the transformed of the structure from amorphous to crystalline after heat treatment at 400 °C. However, the effect of colloidal copper nanoparticles on the deposition rate and hardness of Ni-Cu-P coating deposited by electroless method on L80 steel substrate was not investigated so far. Therefore, in the present study, an attempt was made to create a Ni-Cu-P composite coating by adding colloidal copper nanoparticles. Then the effect of these nanoparticles on the deposition rate as well as the microstructure was investigated. The effect of heat treatment at different temperatures on phase transformations and micro-hardness of the coating was also studied.

Table 1. Chemical compositions of the L80 alloy

Fe	C	Mn	Ni	Cu	P	S	Si
Bal.	0.430	1.900	0.250	0.350	0.030	0.030	0.450

2. Materials and method

2.1. Sample preparation

L80 steel Type 1 (according to API5CT standard) was used as a substrate; Table 1 shows the chemical composition of the alloy. Discs with a diameter of 30 mm and a thickness of 10 mm were prepared for coating. To remove the surface roughness and oxide layers of the samples, sandpaper No. 80 to 1500 was used for ground and polishing. To remove grease and organic contaminants, the samples were immersed in a degreasing solution for 20 min. The degreasing solution composition [4] is brought in Table 2. After that, the samples were washed twice with distilled water and then immersed in 20 wt% HCl solution for 60 s to remove oxide layers and activate the surface. Then the samples were rinsed twice with distilled water and immediately dipped in the electroless plating solution.

Table 2. Chemical composition of degreasing

Chemical composition of degreaser	30 g/L sodium hydroxide, 30 g/L sodium carbonate and 30 g/L sodium phosphate
T (℃)	60
pH	11
t (min)	20

2.2. Preparation of electroless solutions

Nickel sulfate and sodium hypophosphite were used as a source of nickel ions along with a reducing agent and a source of phosphorus, respectively, to make Ni-Cu-P, Ni-P electrolysis solutions. To make a solution containing copper nanoparticles, copper colloidal nanoparticles with 60-70 nm particle size was used. Water solvent and SLS surfactant were utilized in colloidal copper solution with a concentration of 4000 ppm copper nanoparticles. Details of the chemical composition of Ni-Cu-P and Ni-P electroless solutions are given in Table 3. All samples were coated at a temperature of 85±3 °C and a constant pH=4.7±0.2.

Table 3. Chemical compositions of the Ni-P and Ni-Cu-P bath

Bath	$NiSO_4 \cdot 6H_2O$	$Na_2PO_2H_2$	$CH_3COONa.3H_2O$	$C_3H_6O_3$	$Pb(C_2H3O_2)_2$	NH_3	Nano colloid Cu
Electroless Ni-P	32 g/L	30 g/L	38 g/L	28 g/L	1 ppm/ L	5 g/L	-
Electroless Ni-Cu-P	32 g/L	30 g/L	38 g/L	28 g/L	1 ppm/L	5 g/L	0.2,0.3, 0.4 g/L

2.3. Heat treatment

In accordance with ASTM B733 standard for this type of substrate, after coating to improve adhesion and hydrogenation, as well as to transform the initial structure to a crystalline structure, after heat treatment at a temperature of 200 °C for 180 min the samples were exposed to 400 °C for 60 min. The heating rate was 20 °C/min [16].

2.4. Microstructural study of coatings

To identify the copper particle size, a Philips transmission electron microscope (TEM model CM120) was used. To study the type and composition of the phase formed in the coating process and also to study the effect of heat treatment of the samples under phase analysis by Philips XRD (model PW30-40) was used. The diffraction pattern was obtained in the range 2θ=10-90° and step size = 0.05. The voltage used in the device was 30 kW and the applied current was 30 mA. All analyzes used Cu-Kα single radiation with a wavelength of 1.5405 Å. X'Pert High Score software was used to identify the phases. To investigate the chemical composition of the coating, a Cam-Scan field emission microscope equipped (FESEM, model MV2300) equipped with energy dispersive X-ray (EDS) analysis was used.

2.5. Micro-hardness of the coating

A micro-hardness tester made by Beuhler company under the load of 25 g was considered. To obtain a more accurate result from each sample, three points from the top of the coating were considered to take the hardness, and the average hardness number was reported on the micro-Vickers scale.

Table 4. Stability of solution in different amounts of copper nanoparticles

Amount of Cu (mg/l)	Stability condition
-	Stable
0.2	Stable
0.3	Stable
0.4	After 10 min decomposition
0.5	Decomposition immediately

3. Results and discussion

Table 4 shows the stability of electroless Ni-Cu-P solution in different amounts of copper nanoparticles at the same temperature and pH. Electroless baths depend highly on parameters such as temperature, pH, and concentration of bath components [10–13]. If these parameters are not optimal and not controlled, the deposition process will not take place, or the solution will decompose due to a lack of control of free metal ions [16]. When the amount of foreign particles such as copper nanoparticles for compositing exceeds an optimal value, the solution decomposes due to excessive formation of free nickel metal ions and lack of control of these ions by complexing agents. It was found that adding more than 300 mg/L of copper nanoparticles to the solution will lead to solution decomposition. Therefore, 300 mg/L of copper nanoparticles was considered the optimal concentration in all electroless Ni-Cu-P coating samples.

Figure 1 shows a TEM micrograph of colloidal copper particles used in the electroless bath. As it is shown, the size of copper particles is in the range of 60-70 nm and confirms that the nanoparticles copper is a colloidal solution. The presence of nanoparticles increases the strength of the coating through the Orowan mechanism.

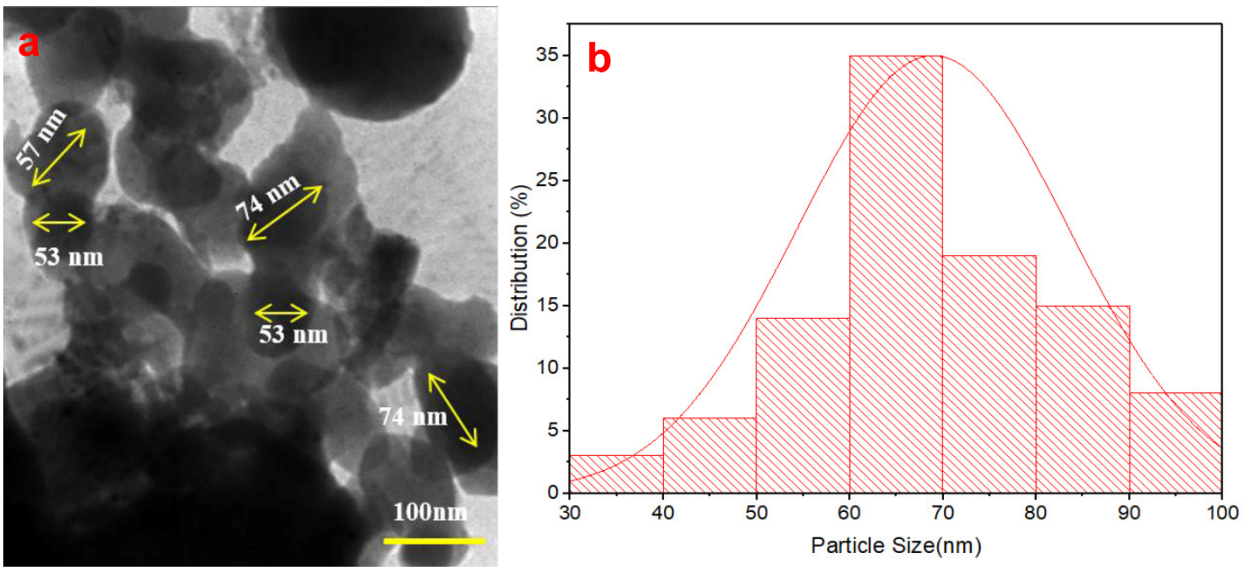

Fig. 1. (a) TEM micrograph of the colloidal copper nanoparticle, and (b) histogram of particle size.

Figure 2 SEM micrographs of the cross-section of Ni-Cup-P and Ni-P electroless coatings deposited at the same conditions (temperature, pH, and stirring speed) for 90 min. According to the obtained thicknesses, the deposition rate in electroless Ni-P and electroless Ni-Cup-P baths is 9.8 and 11 µm/h, respectively. An increase in the deposition rate of a bath containing copper nanoparticles in the bath is related to the copper nanoparticles as an external surface with self-catalytic properties and a high active surface. It should be noted that electroless reactions are catalytic in that the reaction energy is supplied at high temperatures (60 °C ≤ T ≤ 95 °C) [17]. In electroless baths, the surface of the sample and any external agents, including nanoparticles, the wall of the plating chamber, and the elements in the solution play the role of catalyst, and nickel ions tend to deposit on these surfaces [7,8]. In this case, nickel ions approach the surface of these catalysts, and with the reduction conditions created by sodium hypophosphite, nickel ions are reduced to metal. Therefore, in the Ni-Cu-P electroless bath, copper metal nanoparticles, which have a high surface-to-volume ratio, act as a catalyst, resulting in a higher deposition rate than the Ni-P electroless solution. According to Figure 2, it can be seen that in the interface, complete adhesion has been established between the coating and the substrate without any pores. It is evident that a dense coating has been obtained, which increased the corrosion resistance.

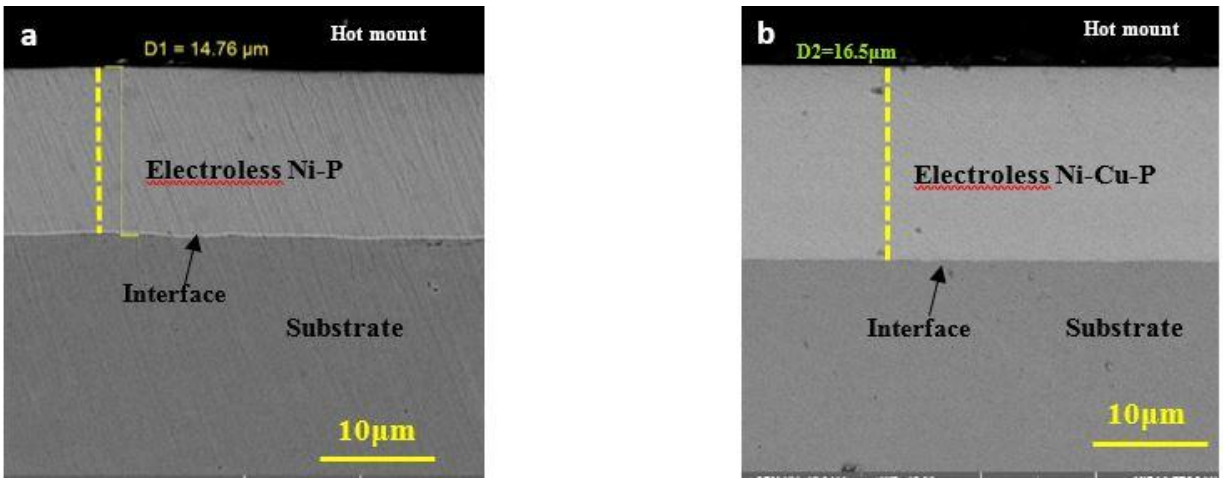

Fig. 2. FESEM micrographs of the cross section of the coating deposition for 90 min: (a) Electroless Ni-P, and (b) Electroless Ni-Cu-P coating.

Figure 3 shows the EDS analysis of electroless Ni-P and electroless Ni-Cu-P coatings. According to the presented chemical composition, the amount of P in both coatings is higher than 10%, and these types are in the category of high phosphorus. On the other hand, the percentage of phosphorus in Ni-Cu-P electroless coating is higher than in Ni-P electroless coating, which shows that the presence of copper nanoparticles, in addition to increasing the deposition rate, could also increase the percentage of phosphorus in the coating. This increase in phosphorus in the Ni-Cu-P coating indicates that the

presence of copper particles causes sodium hypophosphite, which has a reducing and supplying role of phosphorus, to a greater extent in the reduction reaction of nickel ions than in the Ni-P coating. Also, considering that about 300 mg/L of copper nanoparticles were added to the electroless solution as colloidal particles, 4.58wt% or 3.86 at% of these adsorbed particles were detected. Figure 4 EDS map analysis of the electroless Ni-Cu-P coating. As can be seen, the Ni, P, and Cu elements were detected, and uniform distribution of the Ni, P, and Cu elements was achieved. The uniform distribution of copper nanoparticles in the coating can be an advantage of using colloidal copper nanoparticles instead of nanoparticles. In such a way that the copper nanoparticles are uniformly distributed in the solvent containing the surfactant and there is no possibility of its sedimentation by stirring the solution.

(a)

Element	Wt%	At%
Ni	82.85	74.64
Cu	4.85	3.86
P	12.57	21.5

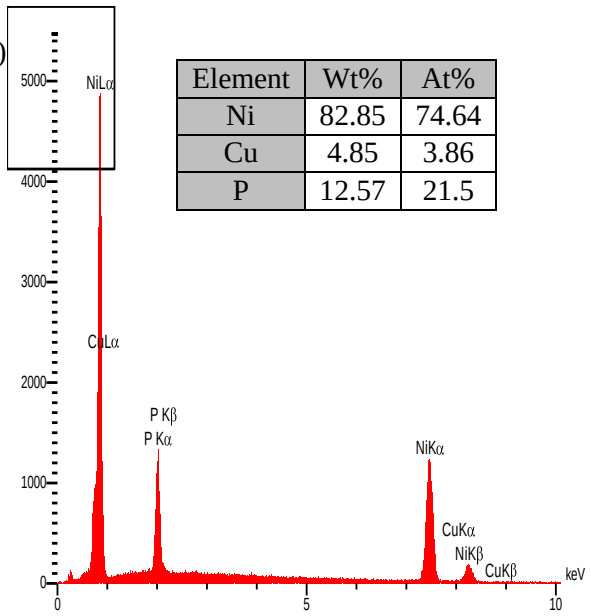

(b)

Element	Wt%	At%
Ni	88.48	80.37
P	11.52	19.63

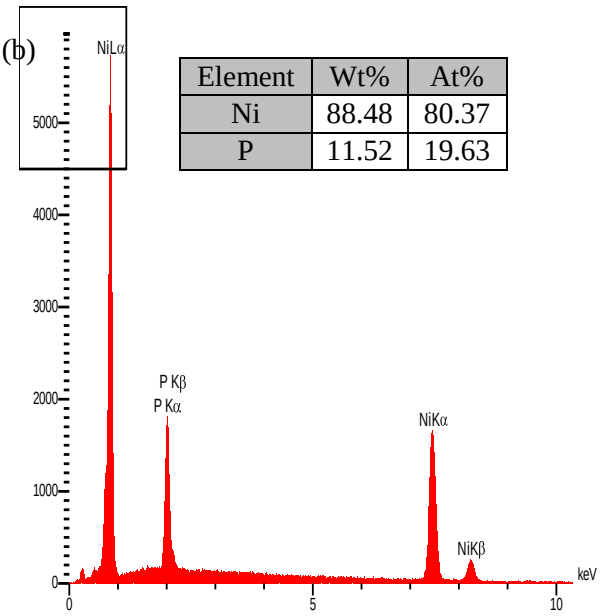

Fig. 3. EDS analysis of the coating: (a) Electroless Ni-P, and (b) Electroless Ni-Cu-P coating

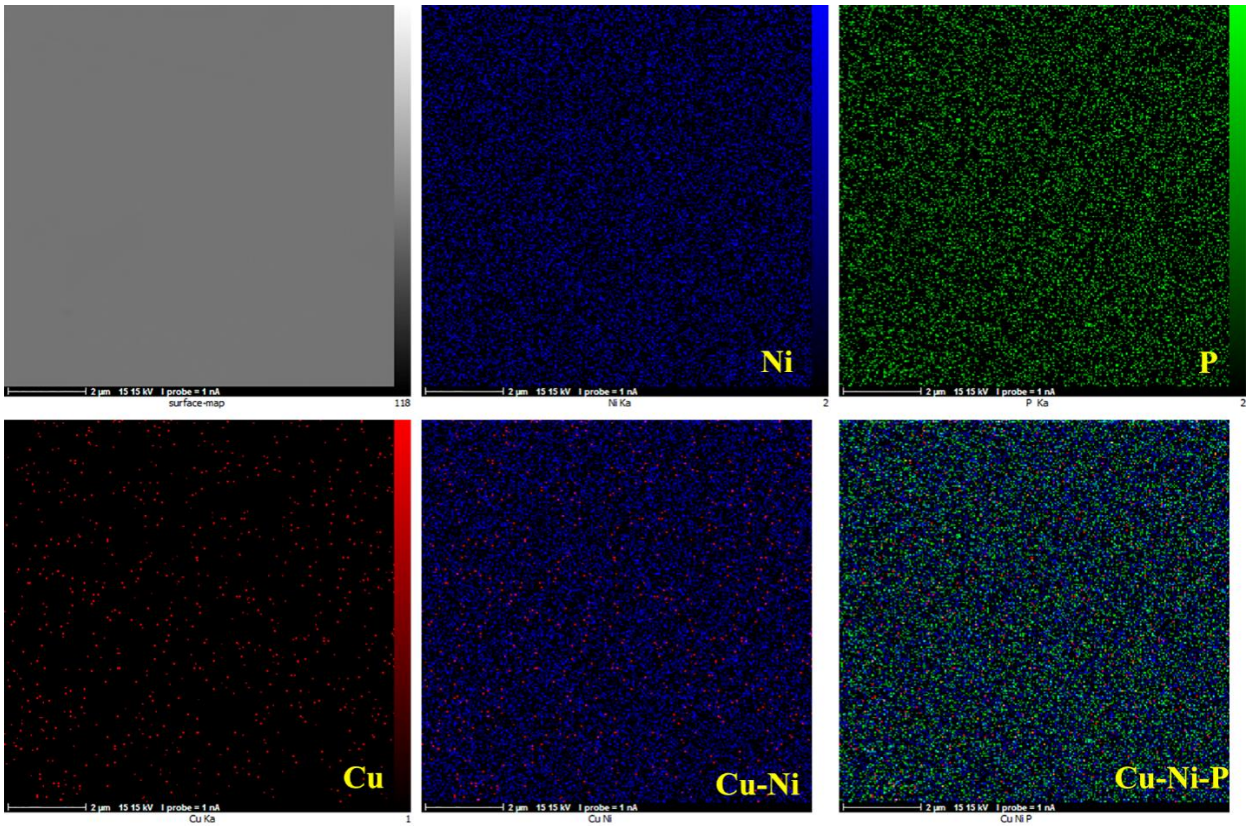

Fig. 4. Elemental map analysis of the Ni-Cu-P coating.

Figure 5 shows the XRD patterns of the electroless Ni-P and Ni-Cu-P coatings before and after heat treatment at 300 °C for 3 h and 400 °C for 1 h. According to the XRD patterns of the samples before heat treatment, both coatings have an amorphous structure, and the presence of copper in the Ni-Cu-P coating has no effect on the crystal microstructure. It is reported that the structural change in the electroless process depends only on the pH and temperature of the electroless bath [16]. On the other hand, heat treatment in both coatings has caused the microstructure to transform to a crystalline state. In this case, the supersaturated amorphous solution in Ni-P coating is transformed to the Ni_{α} and nickel phosphate (Ni_3P) equilibrium phases and in Ni-Cu-P coating transformed to the Ni_{α}, Ni_3P, and $Ni_{3.8}Cu$ phases.

Figure 6 shows the micro-hardness of the electroless Ni-P and Ni-Cu-P coatings after different heat treatments. It can be seen that the micro-hardness of the coatings after heat treatment at 400 °C for Ni-P and Ni-Cu-P coatings was approximately 87% and 73% increase, respectively, compared to before heat treatment. Also, in Ni-Cu-P coating, the presence of copper nanoparticles has increased the hardness. Increased hardness of coatings due to the transformation of the microstructure from amorphous to crystalline during heat treatment and the grain boundaries formation [16, 20]. Furthermore, the presence of Ni_3P phase in Ni-P coating and Ni_3P and $Ni_{3.8}Cu$ phases in Ni-Cu-P coating.

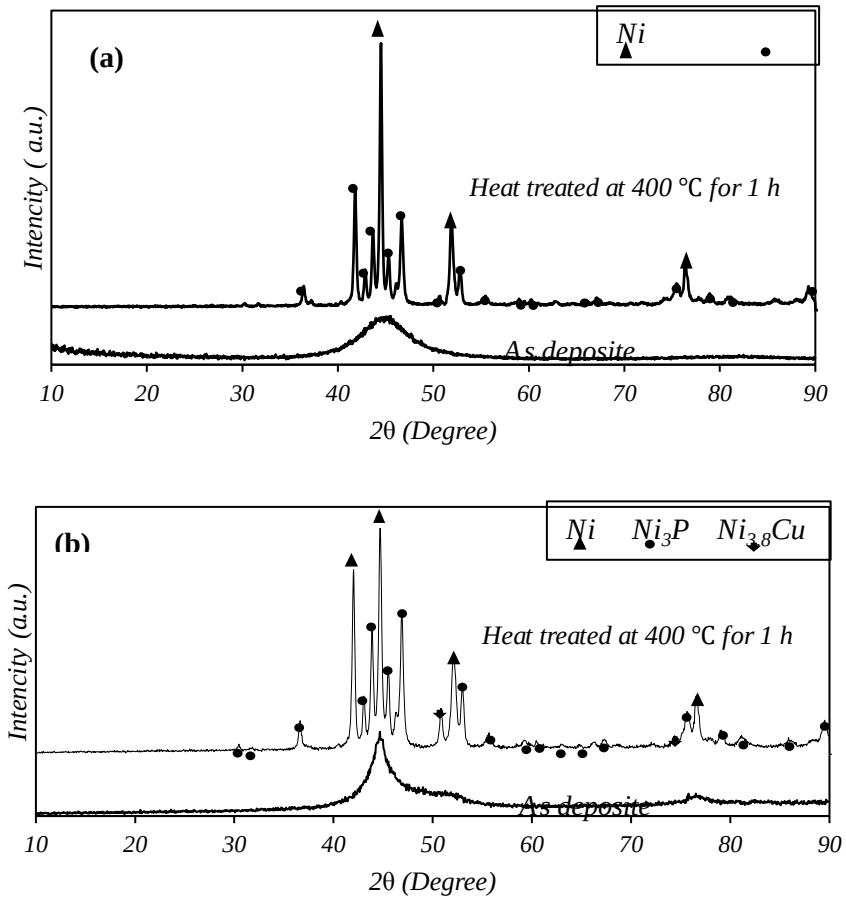

Fig. 5. XRD patterns of the samples before and after heat treatment: (a) Ni-P, and (b) Ni-Cu-P sample.

4. Conclusions

The deposition rate of Ni-Cu-P and Ni-P coatings was applied by the electroless method in an acidic pH bath at 85 °C on an L80 steel substrate was investigated. Experimental results showed that heat treatment at 400 °C and transforming the structure from amorphous to crystalline in both coatings leads to the formation of Ni_{α}, Ni_3P, and $Ni_{3.8}Cu$ phases. Also, colloidal copper nanoparticles in electroless solution, in addition to forming the $Ni_{3.8}Cu$ phase, increase the deposition rate from 10 to 11 µm/h. On the other hand, the presence of copper nanoparticles in the coating before and after heat treatment leads to a significant increase in hardness in the Ni-Cu-P coating compared to the Ni-P coating.

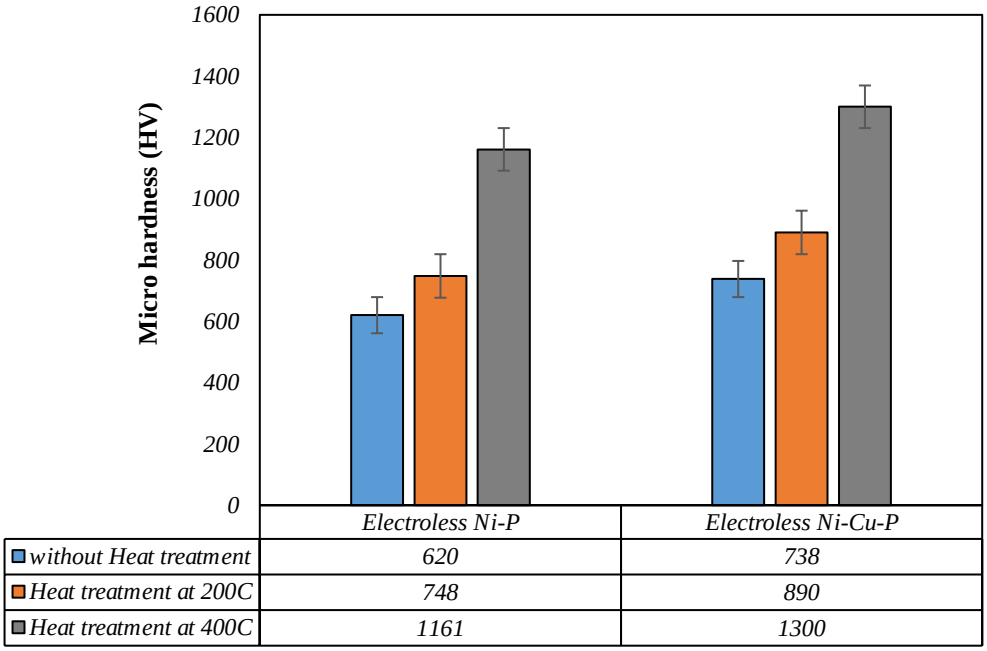

	Electroless Ni-P	Electroless Ni-Cu-P
without Heat treatment	620	738
Heat treatment at 200C	748	890
Heat treatment at 400C	1161	1300

Fig. 6. Micro-hardness of the Ni-P and Ni-Cu-P coating before and after heat treatment.

References

[1] Petroleum and natural gas industries—Steel pipes for use as casing or tubing for wells, Specification for Casing and Tubing API Specification 5CT Eighth Edition, ISO 11960. (2005).

[2] Robert Heidersbach, Metallurgy and Corrosion Control in Oil and Gas Production, John Wiley Sons, Inc. (n.d.), 2018.

[3] F. Bigdeli, M. Javidi, M. Pakshir, A. Khezrloo, M. Tayebi, Risk assessment of the corrosion resistance performances for epoxy coatings under drilling environments using AHP method, Int. J. Press. Vessel. Pip. 193 (2021) 104470.

[4] C. Sun, J. Li, S. Shuang, H. Zeng, J.-L. Luo, Effect of defect on corrosion behavior of electroless Ni-P coating in CO_2-saturated NaCl solution, Corros. Sci. 134 (2018) 23–37.

[5] masoud soltani, A. Shafyei, K. Zarrin naghsh, R. Aliramezani, Effect of Ni-P electroless coating and heat treatment on tribological and corrosion properties of copper substrate, J. Adv. Mater. Process. 6 (2018) 3–13.

[6] D. Davoodi, R. Miri, A.H. Emami, M. Tayebi, S. Salahshour, The effect of NiO catalyst on reduction, synthesis and binder content of TiC-Ni nanocomposite, Int. J. Refract. Met. Hard Mater. 88 (2020) 105175.

[7] J. Sudagar, J. Lian, W. Sha, Electroless nickel, alloy, composite and nano coatings – A critical review, J. Alloys Compd. 571 (2013) 183–204.

[8] A. Chami, B. Nasiri Tabrizi, Effect of heating rate on morphological features of oxidized electroless nickel–boron coatings, J. Adv. Mater. Process. 3 (2015) 61–70.

[9] S.R. Anvari, S.M. Monirvaghefi, M.H. Enayati, Fabrication and characterization of nanostructured functionally graded Ni-P electroless coating, J. Adv. Mater. Process. 4 (2016) 19–29.

[10] I.R. Mafi, C. Dehghanian, Comparison of the coating properties and corrosion rates in electroless Ni–P/PTFE composites prepared by different types of surfactants, Appl. Surf. Sci. 257 (2011) 8653–8658.

[11] A. Arumugam, P. Lakshmanan, S. Palani, K. Parthiban, Wear behavior of Ni-P and Al_2O_3 electroless nano coating on aluminium alloy, Mater. Today Proc. 46 (2021) 1066–1070.

[12] M. Khodaei, A.M. Gholizadeh, SiC nanoparticles incorporation in electroless NiP-Graphene oxide nanocomposite coatings, Ceram. Int. 47 (2021) 25287–25295.

[13] C. Wang, Z. Farhat, G. Jarjoura, M.K. Hassan, A.M. Abdullah, Indentation and bending behavior of electroless Ni-P-Ti composite coatings on pipeline steel, Surf. Coatings Technol. 334 (2018) 243–252.

[14] J. Li, C. Sun, M. Roostaei, M. Mahmoudi, V. Fattahpour, H. Zeng, J.-L. Luo, Characterization and corrosion behavior of electroless Ni-Mo-P/Ni-P composite coating in $CO_2/H_2S/Cl^-$ brine: Effects of Mo addition and heat treatment, Surf. Coatings Technol. 403 (2020) 126416.

[15] S. Du, Z. Li, Z. He, H. Ding, X. Wang, Y. Zhang, Effect of temperature on the friction and wear behavior of electroless Ni–P–MoS2–CaF2 self-lubricating composite coatings, Tribol. Int. 128 (2018) 197–203.

[16] I. Rose, C. Whittington, Nickel Plating

Handbook, Belgium, 2014.
[17] M. Czagany, P. Baumli, Effect of pH on the characteristics of electroless Ni-P coatings, J. Min. Metall. Sect. B Metall. 53 (2017) 20.
[18] F. Tabatabaei, K. Raeissi, A. Saatchi, M. Ürgen, Effect of sodium sulfate on the characteristics and corrosion behavior of high phosphorus Ni–P electroless coatings, Mater. Corros. 65 (2014) 926–930.
[19] S. Kundu, S.K. Das, P. Sahoo, Friction and wear behavior of electroless Ni-P-W coating exposed to elevated temperature, Surfaces and Interfaces. 14 (2019) 192–207.
[20] S. Elahinejad, H. Sharifi, M. Tayebi, A. Rajaee, The influence of nickel coating on the interface of pressureless infiltrated with vibration Al-SiC composites, Mater. Res. Express. 4 (2017) 116506.